Engineering Computations

A contact detection algorithm for superellipsoids based on the common-normal concept

Christian Wellmann, Claudia Lillie, Peter Wriggers,

Received 13 June 2007
Revised 1 February 2008
Accepted 6 February 2008

A contact detection algorithm for superellipsoids based on the common-normal concept

Christian Wellmann, Claudia Lillie and Peter Wriggers
Institute of Mechanics and Computational Mechanics, Leibniz-University of Hannover, Hannover, Germany

Abstract

Purpose – The paper aims to introduce an efficient contact detection algorithm for smooth convex particles.

Design/methodology/approach – The contact points of adjacent particles are defined according to the common-normal concept. The problem of contact detection is formulated as 2D unconstrained optimization problem that is solved by a combination of Newton's method and a Levenberg-Marquardt method.

Findings – The contact detection algorithm is efficient in terms of the number of iterations required to reach a high accuracy. In the case of non-penetrating particles, a penetration can be ruled out in the course of the iterative solution before convergence is reached.

Research limitations/implications – The algorithm is only applicable to smooth convex particles, where a bijective relation between the surface points and the surface normals exists.

Originality/value – By a new kind of formulation, the problem of contact detection between 3D particles can be reduced to a 2D unconstrained optimization problem. This formulation enables fast contact exclusions in the case of non-penetrating particles.

Keywords Computational geometry, Motion

Paper type Research paper

Introduction

Contact detection of moving rigid bodies is an important problem in various fields like discrete element methods (DEMs), computer vision, robotics, etc. When dealing with numerous bodies, the process of contact detection is split into two phases. The goal of the first phase is to reduce the number of inter-particle contact checks from an all-to-all contact check to a considerable smaller number. Typically, spherical or cuboid bounding boxes are defined for each particle and a spatial sorting algorithm is applied to determine the neighbors of each particle. Especially, efficient algorithms for this purpose, which scale linear with the number of particles, can be found in Munjiza *et al.* (2006), Munjiza and Andrews (1998) and Perkins and Williams (2001). In the second phase, a detailed contact check is performed for each pair of adjacent particles. If a contact is detected, the geometric quantities used for the generation of a contact force have to be determined. A broad overview of methods for both parts of the contact detection process is given by Lin and Gottschalk (1998) and Vemuri *et al.* (1998). Obviously, the particle type is crucial for the kind of algorithm that might be applied for the detailed contact check. Particle types can be divided into discrete types consisting of a number of vertices with a corresponding connectivity and continuous types which can be described with the help of implicit or explicit continuous functions.

Engineering Computations: International Journal for Computer-Aided Engineering and Software
Vol. 25 No. 5, 2008
pp. 432-442

0264-4401
DOI 10.1108/02644400810881374

These particle types are further subdivided into convex and non-convex types. Regarding DEMs continuous particles have the advantage of an uniquely defined normal at every surface point, which is favorable for the calculation of contact forces. The simplest kind of continuous particles are spheres for which contact detection is trivial. More sophisticated particle types which were successfully used in DEMs are, e.g. ellipsoids (Ting *et al.*, 1995; Lin and Ng, 1995; Ouadfel and Rothenburg, 1999), the four-arc ellipsoid approximation (Potapov and Campbell, 1998; Wang *et al.*, 1999; Kuhn, 2003; Johnson *et al.*, 2004), and superellipsoids (Barr, 1981; Williams and Pentland, 1992; Cleary *et al.*, 1997). In contrast to the four-arc ellipsoid approximation, ellipsoids and superellipsoids have a continuous curvature, which facilitates the use of a more sophisticated, Hertzian-type contact law.

This paper introduces an efficient algorithm for the second phase of contact detection, that is applicable to any kind of continuous convex particles, that offer an explicit relationship between the surface points and surface normals. The algorithm is described and tested using superellipsoid particles, which offer the greatest variety of shapes among the continuous particles quoted above. It is build as an iterative search for the contact direction, which is the direction parallel to the surface normals at the contact points. In this process, the algorithm exploits the convex shape of the particles by searching for a separating plane, such that each particle lies in a different half-space of the plane. Hence, in the case of non-penetrating particles, it is possible to rule out a penetration before final convergence is reached which reduces the computational effort significantly.

The paper is organized as follows: first, a short introduction of superellipsoids and their important properties regarding the contact detection algorithm is given. Next, the problem of contact detection is formulated as a 2D unconstrained optimization problem in terms of the contact direction. The application of a combined Newton and Levenberg-Marquardt method then leads to the contact detection algorithm. This is followed by an extensive validation of the algorithm and the conclusion.

Superellipsoid

Superellipsoid particles like introduced by Barr (1981) are used, whose definition differs slightly from those used by Williams and Pentland (1992) and Cleary *et al.* (1997). According to Barr (1981), a superellipsoid is described by the so-called inside-outside function:

$$F(x) = \left(\left| \frac{x_1}{r_1} \right|^{2/\epsilon_1} + \left| \frac{x_2}{r_2} \right|^{2/\epsilon_1} \right)^{\epsilon_1/\epsilon_2} + \left| \frac{x_3}{r_3} \right|^{2/\epsilon_2}. \tag{1}$$

Every point x with $F(x) \leq 1$ belongs to the superellipsoid and every point x with $F(x) = 1$ lies on its surface. The radius parameters r_i specify the dimensions of the superellipsoid. The exponents ϵ_1 and ϵ_2 control the squareness of the superellipsoid in the x_1, x_2 plane and x_3 direction, respectively. Here, $\epsilon_i \in (0,2)$ is assumed which leads to a convex body. Note that $\epsilon_i \rightarrow 0$ yields a cuboid and $\epsilon_i \rightarrow 2$ yields an octahedron, compare Figure 1.

Furthermore, it is possible to describe the surface of the superellipsoid in terms of surface parameters ϕ_i through:

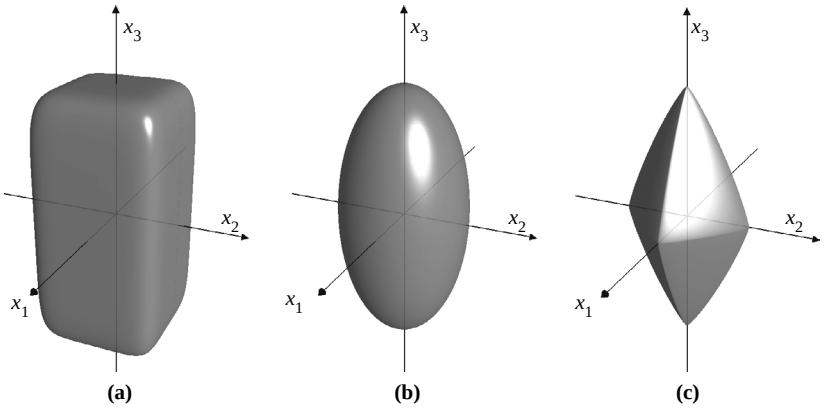

Figure 1.
Superellipsoids with $r_1 = r_2 = r_3/2$ and (a) $\epsilon_i = 0.3$; (b) $\epsilon_i = 1$ and (c) $\epsilon_i = 1.7$

$$x(\phi_1, \phi_2) = \begin{bmatrix} \mathrm{sgn}(\cos\phi_1) r_1 |\cos\phi_1|^{\epsilon_1} |\cos\phi_2|^{\epsilon_2} \\ \mathrm{sgn}(\sin\phi_1) r_2 |\sin\phi_1|^{\epsilon_1} |\cos\phi_2|^{\epsilon_2} \\ \mathrm{sgn}(\sin\phi_2) r_3 |\sin\phi_2|^{\epsilon_2} \end{bmatrix}, \quad \begin{matrix} -\pi \le \phi_1 < \pi \\ -\frac{\pi}{2} \le \phi_2 \le \frac{\pi}{2} \end{matrix}. \tag{2}$$

Regarding the contact detection algorithm, a favorable property of superellipsoids is that the surface normals are easily described in terms of the surface parameters by another superellipsoid equation:

$$\mathbf{n}(\phi_1, \phi_2) = \begin{bmatrix} \mathrm{sgn}(\cos\phi_1)(1/r_1) |\cos\phi_1|^{2-\epsilon_1} |\cos\phi_2|^{2-\epsilon_2} \\ \mathrm{sgn}(\sin\phi_1)(1/r_2) |\sin\phi_1|^{2-\epsilon_1} |\cos\phi_2|^{2-\epsilon_2} \\ \mathrm{sgn}(\sin\phi_2)(1/r_3) |\sin\phi_2|^{2-\epsilon_2} \end{bmatrix}. \tag{3}$$

Hence, there exists a smooth invertible mapping between the 2D space of surface parameters and the 3D space of normalized normal vectors. The surface parameters can be expressed in terms of the normal components $\mathbf{n}_i$ through:

$$\phi_1 = \tan^{-1}\left(s_1 |r_1 \mathbf{n}_1|^{\delta_1}, s_2 |r_2 \mathbf{n}_2|^{\delta_1}\right)$$

$$\phi_2 = \begin{cases} \tan^{-1}\left(|r_1 \mathbf{n}_1|^{\delta_2}, s_3 \left| \left(r_3 \mathbf{n}_3 |\cos\phi_1|^{2-\epsilon_1}\right) \right|^{\delta_2}\right) & \text{if } |r_1 \mathbf{n}_1| > |r_2 \mathbf{n}_2| \\ \tan^{-1}\left(|r_2 \mathbf{n}_2|^{\delta_2}, s_3 \left| \left(r_3 \mathbf{n}_3 |\sin\phi_1|^{2-\epsilon_1}\right) \right|^{\delta_2}\right) & \text{else} \end{cases} \tag{4}$$

$$\text{with} \quad \delta_i = \frac{1}{2 - \epsilon_i}, \quad s_i = \mathrm{sgn}(\mathbf{n}_i).$$

Herein $\tan^{-1}(x, y)$ is the arc tangent of y/x, taking into account which quadrant the point (x,y) is in.

Problem formulation

In DEM simulations, the trajectories of a huge number of particles are determined by application of an explicit time integration scheme to the particles equation of motion. If two particles come into contact, a repulsive contact force has to be applied to prevent them from moving through each over. Typically, the particles are regarded as rigid bodies for the time integration and are considered to be in contact if they inter-penetrate. Repulsive contact forces are then derived from the size of the inter-penetration and chosen in a way to keep the inter-penetration small compared to the size of the particles. A contact detection algorithm therefore has to check if two adjacent particles $\mathscr{P}^1$ and $\mathscr{P}^2$ inter-penetrate and calculate the set of quantities used for contact force generation.

For most of the contact formulations used in DEMs contact points p^1 and p^2, a penetration distance $\mathbf{d} = \|\mathbf{d}\| = \|p^2 - p^1\|$ and a contact direction c belong to this set, compare Figure 2. Regarding the contact force generation, a definition of the contact points based on the common-normal concept is favorable (Johnson, 1985). Accordingly, the contact points are defined as those points that have minimum distance and fulfill:

$$\mathbf{n}^1 = \mu^2 c \quad \mathbf{n}^2 = -\nu^2 c \quad \mathbf{d} \times c = 0. \tag{5}$$

Herein $\mathbf{n}^1$ and $\mathbf{n}^2$ are the outward surface normals at p^1 and p^2 and μ and ν are arbitrary real numbers. Conditions $(5)_1$ and $(5)_2$ assure that the normal vectors are anti-parallel and $(5)_3$ assures that the vector connecting p^1 and p^2 is parallel to the contact direction c.

A number of different approaches have been proposed to calculate the contact quantities listed above. One possibility is to transform equation (5) into a set of non-linear equations in terms of the surface points coordinates by expressing the normal vectors in terms of these coordinates and by elimination of c. Hereat attention has to be paid to multiple solutions, because the minimum distance condition is neglected. This approach was used successfully in combination with ellipsoids (Lin and Ng, 1995) and superellipsoids (Cleary *et al.*, 1997). An approach that only approximately fulfills equation (5) is based on the so-called geometric potential function, which for superellipsoids is the inside-outside function (1) (Ting *et al.*, 1993;

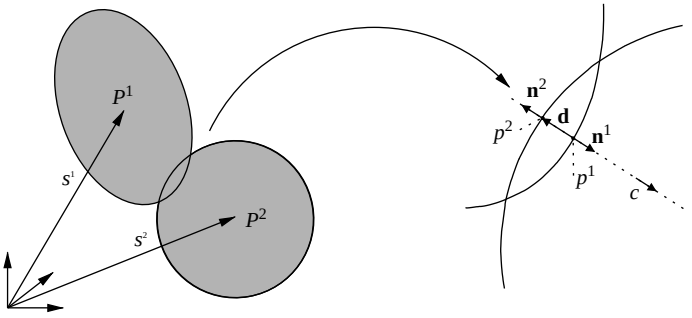

Figure 2.
Two adjacent particles $\mathscr{P}^1$ and $\mathscr{P}^2$ with contact points p^1 and p^2, normal vectors $\mathbf{n}^1$ and $\mathbf{n}^2$, distance vector $\mathbf{d}$ and contact direction c

Lin and Ng, 1995; Tijskens *et al.*, 2004). Lin and Ng (1995), e.g. define the contact points as those points which minimize the geometric potential function of the contact partner. For small penetrations, these methods yield contact points close to that defined by equation (5). Another approximating approach is the discrete function representation approach (Williams and O'Connor, 1995; Hogue, 1998). Here, each particle surface is discretized by a number of points. Contact detection is then done by checking these points for inclusion in the contact partner. This approach allows for a wider range of particle geometries including even some concave geometries. It is performance regarding accuracy and speed depends on the number of points used for the surface discretization.

In the approach presented here, the problem of contact detection is formulated in terms of the contact direction c. For this purpose, the contact direction is parameterized by two angles α_1 and α_2 through:

$$c(\alpha_1, \alpha_2) = \cos\alpha_1 \cos\alpha_2 \, \mathbf{e}_1 + \sin\alpha_1 \cos\alpha_2 \, \mathbf{e}_2 + \sin\alpha_2 \, \mathbf{e}_3$$
$$\text{with } \mathbf{e}_1 = \frac{(\mathbf{s}^2 - \mathbf{s}^1)}{\|\mathbf{s}^2 - \mathbf{s}^1\|} \text{ and } \mathbf{e}_i \cdot \mathbf{e}_j = \delta_{ij}. \tag{6}$$

Herein, the $\mathbf{s}^i$ is the particle center and $(\mathbf{e}_1, \mathbf{e}_2, \mathbf{e}_3)$ are the unit base vectors of a right-handed Cartesian coordinate system with $(\mathbf{e}_1)$ pointing in the direction from the first particle center to the second particle center. As mentioned above for superellipsoids, there exists a smooth invertible mapping between the normal directions and the surface parameters. Hence, the surface points p^1 and p^2 can be determined from α_1 and α_2 so that $(5)_1$ and $(5)_2$ are fulfilled, i.e. the normal vectors $\mathbf{n}^1$ and $\mathbf{n}^2$ at p^1 and p^2 are pointing in opposite directions. For this purpose, the contact direction c has to be transformed into the local coordinate systems of both particles. For each particle, the transformation between the components of local $(\tilde{\bullet})$ and global position and direction vectors is given with the particle center vector $\mathbf{s}$ and it is rotation tensor $\mathbf{T}$ by:

$$x_i = \mathbf{T}_{ij} \tilde{x}_j + s_i \quad \mathbf{d}_i = \mathbf{T}_{ij} \tilde{\mathbf{d}}_j. \tag{7}$$

The surface parameters of p^1 and p^2 can then be determined using equation (4) which finally yields the surface points using equations (2) and (7). Consequently, the distance vector can be expressed in terms of the contact direction angles:

$$\mathbf{d}(\alpha_1, \alpha_2) = p^2(\alpha_1, \alpha_2) - p^1(\alpha_1, \alpha_2). \tag{8}$$

Hence, the problem of contact detection can be formulated as optimization problem in terms of the contact direction angles through:

$$\min_{\alpha_1, \alpha_2} f(\alpha_1, \alpha_2) = \|\mathbf{d}(\alpha_1, \alpha_2)\|^2. \tag{9}$$

Obviously, conditions $(5)_1$ and $(5)_2$ are fulfilled for every direction (α_1, α_2). Furthermore, it can be shown that condition $(5)_3$ is fulfilled at the global minimum of equation (9) if the penetration distance is small compared to the particle sizes and compared to the minimum radius of curvature of the particle surfaces. Hence, the global minimum of

equation (9) yields the contact direction of equation (5) from which the other quantities used for contact force generation can be deducted.

Contact detection algorithm

For an implementation of a contact detection algorithm, any unconstrained optimization algorithm can be applied to problem (9). Here, a combination of Newton's method and a Levenberg-Marquardt method is used. Therefore, the first and second derivatives of f with respect to the contact direction angles have to be determined:

$$f_i = 2(\mathbf{d}\cdot\mathbf{d}_i), \quad f_{ij} = 2(\mathbf{d}_i\cdot\mathbf{d}_j + \mathbf{d}\cdot\mathbf{d}_{ij}) \quad \text{with} \quad \bullet_i = \frac{\partial \bullet}{\partial \alpha_i}. \tag{10}$$

According to equation (8), the derivatives of the distance vector are obtained from the surface points derivatives:

$$\begin{aligned} p_i^\beta &= \frac{\partial p^\beta}{\partial \phi_\gamma}\,\frac{\partial \phi_\gamma}{\partial c_k}\,\frac{\partial c_k}{\partial \alpha_i} \quad p_{ij}^\beta = \frac{\partial^2 p^\beta}{\partial \phi_\gamma \partial \phi_\delta}\,\frac{\partial \phi_\gamma}{\partial c_k}\,\frac{\partial \phi_\delta}{\partial c_l}\,\frac{\partial c_k}{\partial \alpha_i}\,\frac{\partial c_l}{\partial \alpha_j} \\ &+ \frac{\partial p^\beta}{\partial \phi_\gamma}\left(\frac{\partial^2 \phi_\gamma}{\partial c_k \partial c_l}\,\frac{\partial c_k}{\partial \alpha_i}\,\frac{\partial c_l}{\partial \alpha_j} + \frac{\partial \phi_\gamma}{\partial c_k}\,\frac{\partial^2 c_k}{\partial \alpha_i \partial \alpha_j}\right). \end{aligned} \tag{11}$$

Herein, repeated Greek indices denote a summation from 1 to 2 and repeated Latin indices denote a summation from 1 to 3. The single partial derivatives in equation (11) are derived from equations (2), (4), (6) and (7). Care has to be taken because some of the second derivatives $\partial^2 p^\beta/(\partial\phi_\gamma\partial\phi_\delta)$ become indeterminate at points where $\sin\phi_\gamma = 0$ or $\cos\phi_\gamma = 0$. Furthermore, some of the derivatives $\partial\phi_\gamma/\partial c_k$ become indeterminate at points where one or more of the local transforms of the c_k's become zero. In these cases, the points are slightly shifted to compute the gradient and Hessian matrix of f. An iteration step starts with the computation of a search direction $(\mathbf{d}\alpha_1, \mathbf{d}\alpha_2)$ by solving:

$$\begin{bmatrix} f_{11} & f_{12} \\ f_{21} & f_{22} \end{bmatrix} \begin{bmatrix} \mathbf{d}\alpha_1 \\ \mathbf{d}\alpha_2 \end{bmatrix} = - \begin{bmatrix} f_1 \\ f_2 \end{bmatrix} \tag{12}$$

if the Hessian matrix is positive definite. Otherwise, the matrix is modified according to the Levenberg-Marquardt method to guarantee that f decreases in the direction $(\mathbf{d}\alpha_1, \mathbf{d}\alpha_2)$. Next, a step size σ is determined using the Armijo rule and the contact direction angles are updated:

$$^{(i+1)}(\alpha_1, \alpha_2) = {}^{(i)}(\alpha_1, \alpha_2) + \sigma(\mathrm{d}\alpha_1, \mathrm{d}\alpha_2). \tag{13}$$

The iteration stops when a certain accuracy of $\|\mathrm{grad}\, f\| < \mathrm{TOL}$ is reached. An advantage of this approach is that in the case of non-penetrating particles a penetration can be ruled out before the iterative process converges to this accuracy (Figure 3).

In part (a), two adjacent particles are depicted whose bounding boxes intersect. Hence, in a DEM simulation this particle pair will have to be checked for a penetration. Part (b) shows the contact points, normals and the distance vector after i iterations. At this point of the iterative process, a penetration can be ruled out, because it is:

$$ {}^{(i)}\mathbf{n}^1 \cdot {}^{(i)}\mathbf{d} > 0 \Leftrightarrow {}^{(i)}c \cdot {}^{(i)}\mathbf{d} > 0. \tag{14} $$

Because of $(5)_1$, $(5)_2$ and equation (14) ${}^{(i)}p^2$ is the closest point of $\mathscr{P}^2$ to the tangent plane ${}^{(i)}E^1$ with a distance unequal zero. Therefore, ${}^{(i)}E^1$ separates $\mathscr{P}^1$ and $\mathscr{P}^2$ and a penetration can be ruled out. If the criterion (14) is fulfilled for a contact direction ${}^{(i)}c$ the iterative process can be stopped resulting in a significant reduction of the computational effort for contact detection in the case of non-penetrating particles. In the case of a penetration of $\mathscr{P}^1$ and $\mathscr{P}^2$, the algorithm converges to a minimum of f. To ensure that this minimum is the global minimum two conditions have to be checked. First, $(5)_3$ has to be fulfilled. Under the assumption of a small penetration distance, $(5)_3$ can only be fulfilled by a local minimum if the corresponding contact points p_1 and p_2 lie outside $\mathscr{P}^2$ and $\mathscr{P}^1$ (Figure 4).

Hence, the second condition that has to be checked is that $p^1 \in \mathscr{P}^2$ and $p^2 \in \mathscr{P}^1$, which can be done using the inside-outside functions of the particles. If convergence to a local minimum is detected a combination of a random-search method and the Nelder-Mead simplex algorithm (Lagarias *et al.*, 1998) is applied to generate a new start point ${}^{(0)}(\alpha_1, \alpha_2)$. This process is repeated until the global minimum of f is found. In a DEM simulation start values for the direction angles might be drawn from the last time step if a contact pair lasts over multiple time steps. When a contact pair is considered for the first time, the direction of the vector connecting the particle centers is a good initial guess for the contact direction leading to ${}^{(0)}(\alpha_1, \alpha_2) = (0, 0)$, compare equation (6).

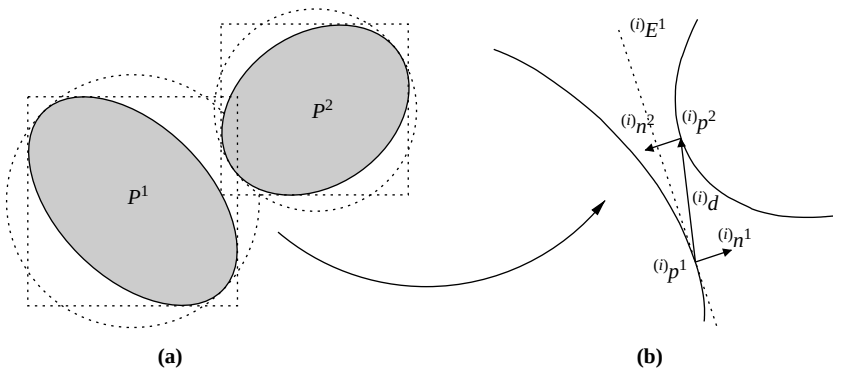

Figure 3.
(a) Two adjacent particles $\mathscr{P}^1$ and $\mathscr{P}^2$ with intersecting spherical and cuboid bounding boxes; (b) contact points, normals and distance vector after i iterations

Note: ${}^{(i)}E^1$ is the tangent plane to $\mathscr{P}^1$ at ${}^{(i)}p^1$

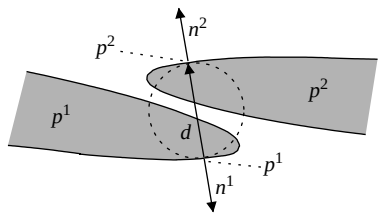

Figure 4.
Two adjacent particles $\mathscr{P}^1$ and $\mathscr{P}^2$ with contact points, normals and distance vector corresponding to a local minimum of f

Note: The dotted circle indicates that d has locally minimum length

Validation

For validation, the contact detection algorithm was applied to a huge number of randomly generated particle pairs. Instead of performing a DEM simulation of an assemblage of particles, each contact pair was generated and checked separately. This has the advantage that due to the generation process the exact solution in terms of the contact direction and the contact points is known so that the solution resulting from the contact detection algorithm can be checked up on its accuracy. Each particle pair was generated according to the following scheme: the first particle center is set to the origin $\mathbf{s}^1 = 0$ and it is rotation tensor is set to the identity tensor $\mathbf{T}^1 = E$. Next, a random contact direction c is generated from which the surface parameters ϕ_i^1 of the contact point p^1 can be determined using equation (4). A random rotation tensor $\mathbf{T}^2$ is generated and the distance $\mathbf{d}$ of the particles is chosen randomly. The second contact point is given as $p^2 = p^1 + \mathbf{d}c$ whereat a positive $\mathbf{d}$ corresponds to a non-penetrating particle pair. The surface parameters ϕ_i^2 of p^2 have to be determined from c and $\mathbf{T}^2$ with the help of equations (4) and (7). Finally, $\mathbf{s}^2$ can be calculated from p^2,ϕ_i^2 and $\mathbf{T}^2$ using equations (2) and (7). The radius parameters r_i of each superellipsoid were chosen randomly and equally distributed from the interval (0.5 and 3.0) yielding a maximum particle aspect ratio of six while the squareness parameters ϵ_i were chosen randomly and equally distributed from one of the intervals listed in Table I.

Two test series were performed where in the first one all particle pairs had a real distance while in the second one they were always in contact. Hence, in the first series the capability of the algorithm for a fast contact exclusion was tested while in the second series the accuracy and efficiency of the algorithm in determining the contact points and direction was tested. For both test series, 10^6 particle pairs were generated for each of the squareness parameter intervals from Table I. The distance of the particles for the first series was chosen randomly and equally distributed from the interval (0, 0.25) and the penetration distance for the second series from the interval $(0, 1.75 \times 10^{-3})$. The direction of the vector connecting the particle centers was always used as initial guess for the contact direction.

In the first test series, the number of iterations needed to rule out a penetration was recorded. The probability of a penetration exclusion after i iterations, which is the number of trials where a penetration was ruled out after i iterations divided by the overall number of trials, is plotted against i in Figure 5. The probability of a penetration exclusion after 0 iterations is 78.2 percent for the squareness parameter Interval 3, 85.2 percent for Interval 2 and 88.1 percent for Interval 1. In this case, the initial guess for the contact direction is good enough to rule out a penetration, so no gradient or Hessian matrix has to be computed. The probability that five or more iterations are needed is 3.7 percent for Interval 3, 1.1 percent for Interval 2 and 1.1 percent for Interval 1. The number of trials where a penetration could not be excluded within 50 iterations is 456 for Interval 3, 24 for Interval 2 and 28 for Interval 1.

Table I. Squareness parameter intervals

Interval No.	1	2	3
$e_{\min}$	1	0.7	0.3
$e_{\max}$	1	1.3	1.7

In these cases, at most three new start points had to be generated until a penetration could be excluded.

In the second test series, the number of iterations to reach an accuracy of $\|\text{grad } f\| < 10^{-6}$ was recorded. The results are shown in Figure 6.

For each squareness parameter interval, convergence is most likely reached after about 2-10 iterations. The probability that 20 or more iterations are needed is 4.5 percent for Interval 3, 0.4 percent for Interval 2 and 0.4 percent for Interval 1. The number of trials where the algorithm converged to a local minimum or did not converge within 50 iterations is 9,219 for Interval 3, 198 for Interval 2 and 193 for Interval 1. Here, at most 15 new start points had to be generated for Intervals 3 and 2 for Intervals 2 and 1.

Finally, the accuracy of the algorithm was analyzed in terms of the relative error of the computed penetration distance $\tilde{\mathbf{d}}$, the distance of the computed and the exact contact points $\tilde{p}^i$ and p^i and the angle between the computed and exact contact direction $\tilde{c}$ and c. The average values for each squareness parameter interval are listed in Table II.

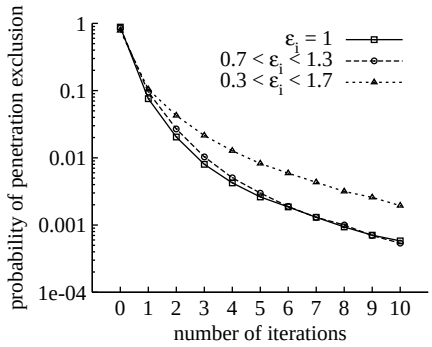

Figure 5.
First test series: probability of a penetration exclusion vs the number of iterations

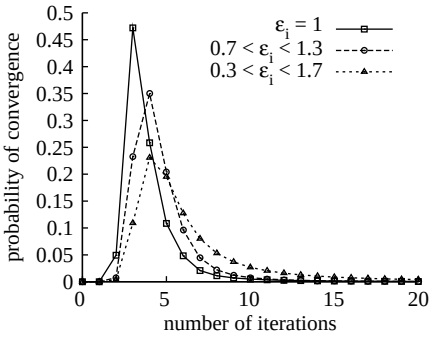

Figure 6.
Second test series: probability to reach convergence vs the number of iterations

Table II.
Average errors of contact detection algorithm results

Interval No.	$\lvert\tilde{\mathbf{d}} - \mathbf{d}\rvert/\mathbf{d}$	$\lVert\tilde{p}^i - p^i\rVert$	Across$(\tilde{c}\cdot c)(\cdot)$
1	2.34×10^{-6}	4.34×10^{-8}	4.21×10^{-3}
2	2.40×10^{-6}	4.40×10^{-8}	5.05×10^{-3}
3	3.21×10^{-5}	3.72×10^{-7}	1.82×10^{-2}

Conclusion

A contact detection algorithm is introduced that is applicable to convex continuous particles, which offer an explicit relationship between contact normals and surface points. The main characteristic of the algorithm is that it searches for the contact direction instead of the contact points. This, in combination with the convex particle shape, offers the possibility of a penetration exclusion before final convergence is reached. Numerical tests showed that a fast penetration exclusion is very probable yielding a high efficiency of the algorithm when applied to non-penetrating particle pairs. In the case of a penetration, the algorithm most likely converges in less than ten iterations yielding a high accuracy in terms of the penetration distance, contact points and contact direction. Therefore, the algorithm is expected to show good performance when applied to DEM simulations of convex continuous particles.

References

Barr, A.H. (1981), "Superquadrics and angle-preserving transformations", *IEEE Computer Graphics and Applications*, Vol. 1 No. 1, pp. 11-23.

Cleary, P.W., Stokes, N. and Hurley, J. (1997), "Efficient collision detection for three dimensional super-ellipsoidal particles", *Proceedings of 8th International Computational Techniques and Applications Conference CTAC97, Adelaide*.

Hogue, C. (1998), "Shape representation and contact detection for discrete element simulations of arbitrary geometries", *Engineering Computations*, Vol. 15 No. 3, pp. 374-90.

Johnson, K.L. (1985), *Contact Mechanics*, Cambridge University Press, Cambridge.

Johnson, S., Williams, J.R. and Cook, B. (2004), "Contact resolution algorithm for an ellipsoid approximation for discrete element modeling", *Engineering Computations*, Vol. 21 Nos 2/3/4, pp. 215-34.

Kuhn, M.R. (2003), "Smooth convex three-dimensional particle for the discrete-element method", *Journal of Engineering Mechanics*, Vol. 129 No. 5, pp. 539-47.

Lagarias, J.C., Reeds, J.A., Wright, M.H. and Wright, P.E. (1998), "Convergence properties of the nelder-mead simplex algorithm in low dimensions", *SIAM Journal on Optimization*, Vol. 9, pp. 112-47.

Lin, M.C. and Gottschalk, S. (1998), "Collision detection between geometric models: a survey", *Proceedings of IMA Conference on Mathematics of Surfaces*.

Lin, X. and Ng, T-T. (1995), "Contact detection algorithms for three-dimensional ellipsoids in discrete element modelling", *International Journal for Numerical and Analytical Methods in Geomechanics*, Vol. 19 No. 9, pp. 653-9.

Munjiza, A. and Andrews, K.R.F. (1998), "NBS contact detection algorithm for bodies of similar size", *International Journal for Numerical Methods in Engineering*, Vol. 43, pp. 131-49.

Munjiza, A., Rougier, E. and John, N.W.M. (2006), "MR linear contact detection algorithm", *International Journal for Numerical Methods in Engineering*, Vol. 66, pp. 46-71.

Ouadfel, H. and Rothenburg, L. (1999), "An algorithm for detecting inter-ellipsoid contacts", *Computers and Geotechnics*, Vol. 24 No. 4, pp. 245-63.

Perkins, E. and Williams, J.R. (2001), "A fast contact detection algorithm insensitive to object sizes", *Engineering Computations*, Vol. 18 Nos 1/2, pp. 48-61.

Potapov, A.V. and Campbell, C.S. (1998), "A fast model for the simulation of non-round particles", *Granular Matter*, Vol. 1 No. 1, pp. 9-14.

Tijskens, E., de Baerdemaeker, J. and Ramon, H. (2004), "Strategies for contact resolution of level surfaces", *Engineering Computations*, Vol. 21 Nos 2/3/4, pp. 137-50.

Ting, J.M., Khwaja, M., Meachum, L.R. and Rowell, J.D. (1993), "An ellipse-based discrete element model for granular materials", *International Journal for Numerical and Analytical Methods in Geomechanics*, Vol. 17 No. 9, pp. 603-23.

Ting, J.M., Meachum, L.R. and Rowell, J.D. (1995), "Effect of particle shape on the strength and deformation mechanisms of ellipse-shaped granular assemblages", *Engineering Computations*, Vol. 12 No. 2, pp. 99-108.

Vemuri, B.C., Cao, Y. and Chen, L. (1998), "Fast collision detection algorithms with applications to particle flow", *Computer Graphics Forum*, Vol. 17 No. 2, pp. 121-34.

Wang, C-Y., Wang, C-F. and Sheng, J. (1999), "A packing generation scheme for the granular assemblies with 3D ellipsoidal particles", *International Journal for Numerical and Analytical Methods in Geomechanics*, Vol. 23 No. 8, pp. 815-28.

Williams, J.R. and O'Connor, R. (1995), "A linear complexity intersection algorithm for discrete element simulation of arbitrary geometries", *Engineering Computations*, Vol. 12 No. 2, pp. 185-201.

Williams, J.R. and Pentland, A.P. (1992), "Superquadrics and modal dynamics for discrete elements in interactive design", *Engineering Computations*, Vol. 9 No. 2, pp. 115-27.

Corresponding author
Christian Wellmann can be contacted at: wellmann@ibnm.uni-hannover.de

This article has been cited by:

1. T.I. Zohdi. 2018. Laser-induced heating of dynamic particulate depositions in additive manufacturing. *Computer Methods in Applied Mechanics and Engineering* **331**, 232-258. [Crossref]
2. Kamyar Kildashti, Kejun Dong, Bijan Samali, Qijun Zheng, Aibing Yu. 2018. Evaluation of contact force models for discrete modelling of ellipsoidal particles. *Chemical Engineering Science* **177**, 1-17. [Crossref]
3. Kamyar Kildashti, Kejun Dong, Bijan Samali. 2018. A revisit of common normal method for discrete modelling of non-spherical particles. *Powder Technology* **326**, 1-6. [Crossref]
4. Sven Stühler, Florian Fleissner, Peter Eberhard. 2018. A contact detection algorithm for deformable tetrahedral geometries based on a novel approach for general simplices used in the discrete element method. *Computational Particle Mechanics* **5**:1, 35-47. [Crossref]
5. Artur Alves Gonçalves, Alexandre Bernardino, Joaquim Jorge, Daniel Simões Lopes. 2017. A benchmark study on accuracy-controlled distance calculation between superellipsoid and superovoid contact geometries. *Mechanism and Machine Theory* **115**, 77-96. [Crossref]
6. Rafael Bravo, Pablo Ortiz, José Luis Pérez–Aparicio. 2017. Analytical and discrete solutions for the incipient motion of ellipsoidal sediment particles. *Journal of Hydraulic Research* **103**, 1-15. [Crossref]
7. T.I. Zohdi. 2017. Computational modeling of electrically-driven deposition of ionized polydisperse particulate powder mixtures in advanced manufacturing processes. *Journal of Computational Physics* **340**, 309-329. [Crossref]
8. Alfredo Gay Neto, Paulo M. Pimenta, Peter Wriggers. 2017. A master-surface to master-surface formulation for beam to beam contact. Part II: Frictional interaction. *Computer Methods in Applied Mechanics and Engineering* **319**, 146-174. [Crossref]
9. Shiwei Zhao, Xiaowen Zhou. 2017. Effects of particle asphericity on the macro- and micro-mechanical behaviors of granular assemblies. *Granular Matter* **19**:2. . [Crossref]
10. Shiwei Zhao, Nan Zhang, Xiaowen Zhou, Lei Zhang. 2017. Particle shape effects on fabric of granular random packing. *Powder Technology* **310**, 175-186. [Crossref]
11. Li Xin Xu. 2017. A method for modelling contact between circular and non-circular shapes with variable radii of curvature and its application in planar mechanical systems. *Multibody System Dynamics* **39**:3, 153-174. [Crossref]
12. Urtė Radvilaitė, Álvaro Ramírez-Gómez, Rimantas Kačianauskas. 2016. Determining the shape of agricultural materials using spherical harmonics. *Computers and Electronics in Agriculture* **128**, 160-171. [Crossref]
13. . Non-Spherical Particles 152-188. [Crossref]
14. T.I. Zohdi. 2016. On progressive blast envelope evolution of charged particles in electromagnetic fields. *Computer Methods in Applied Mechanics and Engineering* **308**, 47-72. [Crossref]
15. D. S. Lopes, R. R. Neptune, J. A. Ambrósio, M. T. Silva. 2016. A superellipsoid-plane model for simulating foot-ground contact during human gait. *Computer Methods in Biomechanics and Biomedical Engineering* **19**:9, 954-963. [Crossref]
16. C. R. K. Windows-Yule, D. R. Tunuguntla, D. J. Parker. 2016. Numerical modelling of granular flows: a reality check. *Computational Particle Mechanics* **3**:3, 311-332. [Crossref]
17. T. I. Zohdi. 2016. A discrete element and ray framework for rapid simulation of acoustical dispersion of microscale particulate agglomerations. *Computational Mechanics* **57**:3, 465-482. [Crossref]

18. T.I. Zohdi. 2016. Modeling and efficient simulation of the deposition of particulate flows onto compliant substrates. *International Journal of Engineering Science* **99**, 74-91. [Crossref]
19. Lin Chen, Chongqi Ni, Junjie Feng, Jun Dai, Bingqiong Huang, Huaping Liu, Haihong Pan. 2015. Proximity query based on second order cone programming using convex superquadrics: a static collision detection algorithm for narrow-phase. *Assembly Automation* **35**:4, 367-375. [Abstract] [Full Text] [PDF]
20. D. Höhner, S. Wirtz, V. Scherer. 2015. A study on the influence of particle shape on the mechanical interactions of granular media in a hopper using the Discrete Element Method. *Powder Technology* **278**, 286-305. [Crossref]
21. G. Lu, J.R. Third, C.R. Müller. 2015. Discrete element models for non-spherical particle systems: From theoretical developments to applications. *Chemical Engineering Science* **127**, 425-465. [Crossref]
22. T. I. Zohdi. 2014. Additive particle deposition and selective laser processing-a computational manufacturing framework. *Computational Mechanics* **54**:1, 171-191. [Crossref]
23. T. Zohdi. 2014. Embedded electromagnetically sensitive particle motion in functionalized fluids. *Computational Particle Mechanics* **1**:1, 27-45. [Crossref]
24. D. Höhner, S. Wirtz, V. Scherer. 2014. A study on the influence of particle shape and shape approximation on particle mechanics in a rotating drum using the discrete element method. *Powder Technology* **253**, 256-265. [Crossref]
25. R. Bravo, J.L. Pérez-Aparicio, T.A. Laursen. 2012. An energy consistent frictional dissipating algorithm for particle contact problems. *International Journal for Numerical Methods in Engineering* **92**:9, 753-781. [Crossref]
26. B. Avci, P. Wriggers. 2012. A DEM-FEM Coupling Approach for the Direct Numerical Simulation of 3D Particulate Flows. *Journal of Applied Mechanics* **79**:1, 010901. [Crossref]
27. Christian Wellmann, Peter Wriggers. 2012. A two-scale model of granular materials. *Computer Methods in Applied Mechanics and Engineering* **205-208**, 46-58. [Crossref]
28. A. Pazouki, H. Mazhar, D. Negrut. 2012. Parallel collision detection of ellipsoids with applications in large scale multibody dynamics. *Mathematics and Computers in Simulation* **82**:5, 879-894. [Crossref]
29. Martin Obermayr, Klaus Dressler, Christos Vrettos, Peter Eberhard. 2011. Prediction of draft forces in cohesionless soil with the Discrete Element Method. *Journal of Terramechanics* **48**:5, 347-358. [Crossref]
30. Darius Markauskas, Rimantas Kačianauskas. 2011. Investigation of rice grain flow by multi-sphere particle model with rolling resistance. *Granular Matter* **13**:2, 143-148. [Crossref]
31. Daniel S. Lopes, Miguel T. Silva, Jorge A. Ambrósio, Paulo Flores. 2010. A mathematical framework for rigid contact detection between quadric and superquadric surfaces. *Multibody System Dynamics* **24**:3, 255-280. [Crossref]
32. Paulo Flores, Jorge Ambrósio. 2010. On the contact detection for contact-impact analysis in multibody systems. *Multibody System Dynamics* **24**:1, 103-122. [Crossref]
33. D. Markauskas, R. Kačianauskas, A. Džiugys, R. Navakas. 2010. Investigation of adequacy of multi-sphere approximation of elliptical particles for DEM simulations. *Granular Matter* **12**:1, 107-123. [Crossref]